

1 **Simple preparation and initial characterization**
2 **of semi-amorphous hollow calcium silicate**
3 **hydrate nanoparticles by ammonia-**
4 **hydrothermal-template techniques**

5 Raymond V.Rivera Virtudazo, Hideo Watanabe, Takashi Shirai, Masayoshi Fuji*

6 *Advanced Ceramics Research Center, Nagoya Institute of Technology,*
7 *Crystal Plaza 4F, 3-101-1 Honmachi, Tajimi, Gifu 507-0033 Japan*

8 Tel.: +81-572-24-8110

9 Fax: +81-572-24-8109

10 *corresponding author: fuji@nitech.ac.jp

11

12 Email addresses:

13 RVRV: raymond@crl.nitech.ac.jp or rrvv26@gmail.com

14 H.W: hideo.watanabe@gmail.com

15 T.S: shirai@nitech.ac.jp

16 M.F: fuji@nitech.a.jp

17

18 Article note:

19

20

21

22

23

24

25

26

27

28

29

30

31

32

33

34

1 **Abstract**

2 Semi-amorphous hollow calcium silicate hydrate nanoparticles (CS10d120Hac)
3 were successfully synthesized via simple ammonia-hydrothermal template
4 approach (AHT) followed by acid treatment. Results revealed that the newly
5 synthesized samples had homogenous hollow nano-interior wherein the shell-wall
6 contained semi-amorphous calcium silicate hydrate. The AHT intensified the
7 formation of a stronger electrostatic interaction (Si-O-Ca) from the weaker
8 electrostatic contact composed of silicate wall-calcium hydroxide interaction (Si-
9 OH-Ca) forming a thin semi-amorphous calcium silicate hydrate shell wall. This
10 is also a convenient way for structural stability of the hollow calcium silicate
11 hydrate nanoparticle (CS10d120Hac). The CS10d120Hac showed a relatively
12 higher surface area, which is uniquely rare especially if compared with bulk
13 calcium silicate particles. This CS10d120Hac can be selectively functionalized
14 with multiple organic and inorganic groups. Hence, this work may open a new
15 route for the formation of hybrid hollow bio-active particles.

16 **Keywords** Calcium silicate hydrate, Hollow nanoparticles, Colloidal,
17 Hydrothermal-template synthesis

18
19
20
21
22
23
24
25
26
27
28
29
30
31
32
33
34

1 **Introduction**

2 Recently, nanosize calcium silicate hydrate (CSH) materials have been
3 increasingly significant because of its potential function in the field of nano-
4 medicine and cement science applications (Gandolfi et al. 2010; Wu et al. 2010;
5 Chen et al. 2011). CSH possesses a remarkable level of structural stability, which
6 is about more than 30 crystalline CSH excluding the amorphous CSH, and are
7 described as generic term CSH (Taylor 1986). The composition varies with no
8 specific range and is usually prepared by hydrothermal process (HP), wherein the
9 structures can be in a range of semi-crystalline to nearly amorphous structure. The
10 synthesis of CSH microfibers via HP, subjected to high temperature reaction at
11 180 to 350 °C, was successfully done (Mitsuda et al. 1986; Udawatte et al. 2000;
12 Watanabe et al. 2001; Rios et al. 2009; Nicoleau 2010). Moreover, some
13 researchers also attempted to form a bone-like CSH-apatite-like material with
14 hollow microspheres for drug delivery applications (DDA) (Li et al. 2005;
15 Gandolfi et al. 2010; Wu et al. 2010; Zhang et al. 2010) but the synthesized CSH
16 particles were too large, hierarchically not well defined, unstable, of non-uniform
17 particle size, and were produced in low quantity from a technically complicated
18 process. Accordingly, in order to maximize the full potential of CSH materials for
19 bio-activity and DDA, a large specific surface area with a relatively higher pore
20 volume, lower density, and well-defined interconnected pore networks are desired
21 and precisely significant (Okada et al. 1994; Huang et al. 2002; Saravanapavan et
22 al. 2003; Gou et al. 2004; Allen et al. 2007; Coleman et al. 2007; Pei et al. 2010).
23 One strategy is to produce nanosize CSH phase material with porous shell wall
24 and hollow interior structures that could lead to superior nano-bio-active material
25 or nano-cement applications. This type of CSH nano-material is usually difficult
26 to prepare using the most common processes (such as nano-emulsion, sono-

1 chemical, etc). For this reason, the development of a general and simple method
2 for the preparation of hollow CSH nanoparticles is needed so that the surfaces can
3 be easily modified and can be used for practical-novel applications. Up to now,
4 the attempt to fabricate semi-amorphous hollow CSH nanoparticles
5 (CS10d120Hac) is still a challenge and this new type of CSH nanoparticles has
6 not yet been fully reported.

7 To address this issue we used our previous research on colloidal core-shell
8 $\text{CaCO}_3@\text{SiO}_2$ (calcium-silicate system) nanoparticles (Shin et al. 2003; Fuji et al.
9 2007; Virtudazo et al. 2010) followed by aging by solvothermal concept (SC) to
10 form CSH phase nano-materials (Chippindale et al. 1996; Devaraju et al. 2009;
11 Chang et al. 2010; Blakely et al. 2011). Fabricating the nano-CSH shell structure
12 via SC is a convenient method to produce this type of materials (Udawatte et al.
13 2000; Takagi et al. 2009; Nicoleau 2010). The SC process is done by heating the
14 solution (sample with solvent) above its boiling point contained in a sealed vessel
15 (such as an autoclave container) wherein the pressure autogenously far exceeds
16 the ambient pressure. In this process, the autoclave in an aqueous ammonia
17 solution with core-shell particles designate as the ammonia-hydrothermal template
18 method (AHT) (Lin et al. 1999, 2000, 2001). This process exploits the measurable
19 solubility and reactivity of the inorganic substances in the solvent at elevated
20 temperature and pressure. Moreover, it permits subsequent partial crystallization
21 of the dissolve precursor ions during the AHT process. Hence, complex structures
22 (such as CSH) may occur in AHT. Generally, the reaction temperature, solvent
23 and concentration are some of the parameters that can be readily altered in AHT.

24 In this paper, we report a novel type, eco-friendly, surfactant-free and non-toxic
25 method to fabricate semi-amorphous CS10d120Hac via AHT followed by
26 dissolution of CaCO_3 core-nanoparticles from the colloidal solution composed of

1 composite core-shell ($\text{CaCO}_3@\text{SiO}_2$) nanoparticles. The CS10d120Hac produced
2 is a relatively uniform nanosize hollow particles ranging from (60 to 100) nm with
3 a stable surface morphology, composed of ultra microporous shell wall. It
4 contains an external and internal surface that can be selectively functionalized
5 with multiple organic and inorganic groups. Henceforth, this work may open a
6 new route to prepare hybrid hollow bio-active particles.

7 **Experimental**

8 **Materials**

9 Nanocube 60 calcium carbonate (CaCO_3 , Nittetsu Mining Co., Ltd Japan),
10 tetraethoxysilane (TEOS, Wako Pure Chemical Industries, Ltd., > 95 %),
11 ammonia water (NH_4OH , Wako Pure Chemical Industries, Ltd., >28 %) and
12 ethanol (EtOH ($\text{CH}_3\text{CH}_2\text{OH}$), Wako Pure Chemical Industries, Ltd., > 99.8 %)
13 were used as received.

14 **Synthesis of core-shell CSH nanoparticles**

15 The synthesis was based on our previous works (Virtudazo et al. 2010; Fuji et al.
16 2011; Takai et al. 2011) with the addition of AHT during the reaction. In this
17 procedure, 3.29 g of CaCO_3 nanocube particles was dispersed in 15.52 mL of
18 EtOH and continuously stirred for 10 min at room temperature (RT) using an
19 ultrasonic. Then 1 mL of TEOS was slowly added to the solution, followed by 1
20 mL of $\text{NH}_4\text{OH}_{\text{aq}}$. The white slurry was continuously stirred for 2 h, then obtained
21 a composite core-shell $\text{CaCO}_3@\text{SiO}_2$ nanoparticles with a typical molar ratio of
22 7.3:58.9:1:7.8:3.4 (CaCO_3 : EtOH: TEOS: H_2O : NH_3). After 2 h, the slurry was
23 transferred to a 50 mL-autoclaveable, Teflon-lined stainless steel with an
24 estimated pressure of 50 kg cm^{-2} . This was heated to 120°C for 10 d. After 10 d

1 aging, the vessel was cooled to RT and then synthesized product was filtered and
2 washed several times with EtOH/H₂O mixture until neutral. The composite core-
3 shell calcium silicate hydrate nanoparticles (CSH nanoparticles) were then dried
4 in a vacuum oven at 90 °C for 5 h.
5 (*Note* During AHT, the temperature reactions were varied from RT (no
6 hydrothermal; HS0dAH0ac), 90 °C for 10 d (HS10d90Hac), and 120 °C for 10 d
7 (CS10d120Hac)).

8 **Fabrication of hollow CSH nanoparticles**

9 To obtain hollow particles, 0.7 g of dried powder sample (all as-synthesized dried
10 core-shell nanoparticles) was subjected to acid treatment using 15 mL of 3 mol L⁻¹
11 HCl with continuous stirring for 8 h at RT. The mixture was then filtered and
12 washed several times (until neutral) with EtOH/H₂O mixture. The obtained glassy
13 gel solid (hollow) was vacuum dried at 90 °C for 1 d. The hollow nano-size
14 particles obtained were named as follows: HS0dAHOac, HS10d90Hac and
15 CS10d120Hac. The process flow for the formation of (CS10d120Hac) hollow
16 CSH nanoparticles is illustrated in Fig. 1.

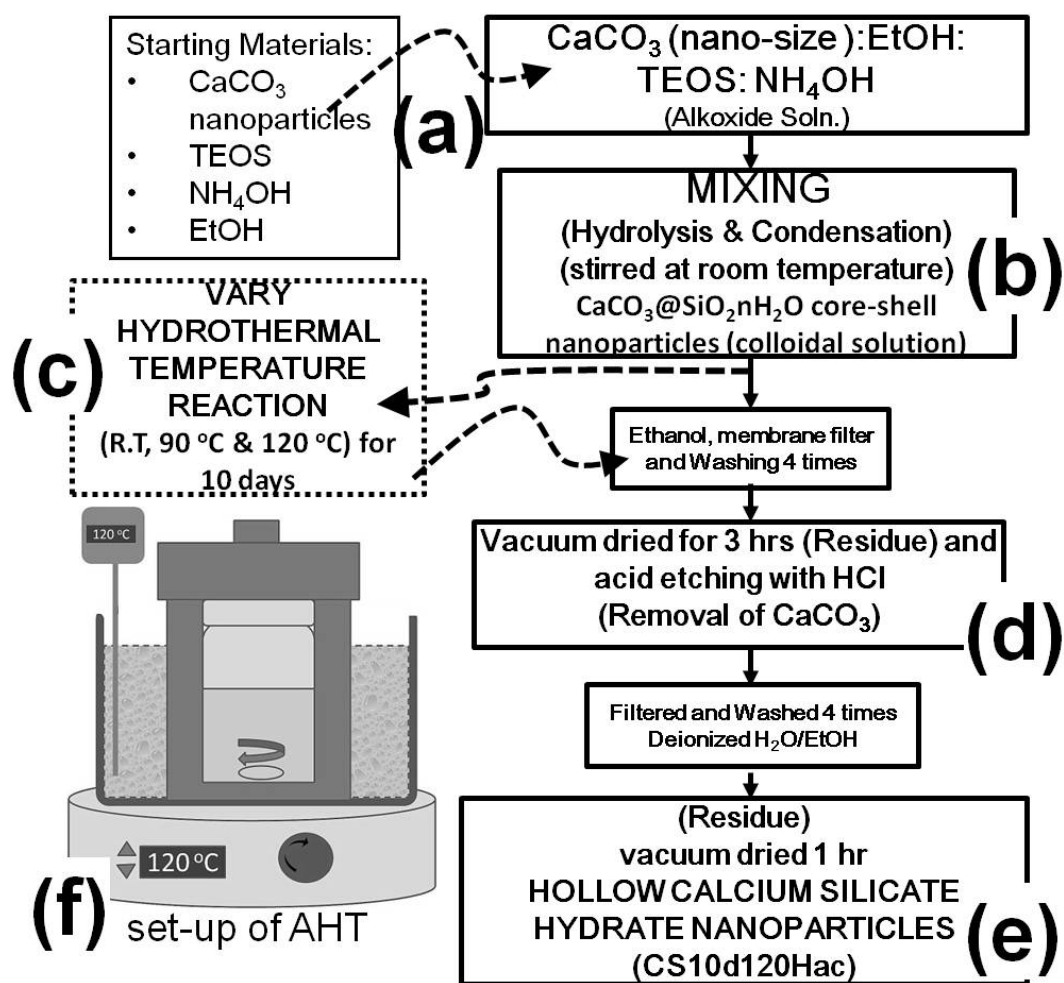


Fig. 1 Process flow with an illustration of the simple set-up of AHT (f) during the synthesis of CS10d120Hac: **a** proportioning; **b** mixing for hydrolysis and condensation to form core-shell nanoparticles ($\text{CaCO}_3@\text{SiO}_2.n\text{H}_2\text{O}$); **c** subjected to AHT at varying temperature for 10 days; **d** Dried and acid etched to remove CaCO_3 nanoparticles templates; **e** then obtain CS10d120Hac

Characterization

The products were characterized by X-ray Diffraction (XRD, Model RINT 1100, Rigaku) with $\text{Cu K}\alpha$ radiation ($\lambda = 1.54056 \text{ \AA}$) at a scanning rate of $0.02^\circ \text{ s}^{-1}$ ($5^\circ - 60^\circ$, 2θ) with an operating voltage of 40 kV and emission current 40 mA. The thermal property of the sample was investigated using thermogravimetry (TG, TG-8120, Rigaku, Japan) under oxygen atmosphere. The temperature was increased at a rate of $10^\circ \text{C min}^{-1}$ from 22 to 1000°C . Morphology and microstructure of the hollow particles were examined using scanning electron

1 microscopy (SEM; JSM-7000F, JEOL) and transmission electron microscopy
2 (TEM, 2000EXII). The specific surface area and cavity-pore size distribution of
3 the hollow samples were determined by Brunauer-Emmett-Tellers (BET) method
4 and Barrett-Joyner-Halenda (BJH) method, respectively via the automatic surface
5 area analyzer (BELSORP-max) using Nitrogen gas (N_2) adsorption desorption
6 isotherm recorded at 77 K.

7 **Results and discussions**

8 Figure 1 illustrates the process for producing CS10d120Hac via AHT. Core-shell
9 nanoparticles were formed during hydrolysis of TEOS (a siloxane) followed by
10 condensation of silicate which coated the core- $CaCO_3$ nanoparticles. The colloidal
11 solution was then subjected to AHT with aging and followed by acid-etching.

12 **Crystallographic properties**

13 Using the x-ray diffraction patterns (XRD), the results showed a diffraction angle
14 identified as calcite (core nanoparticles $CaCO_3$) (Hoshino, et al. 2006; Fuji, et al.
15 2007). This was clearly shown for the samples such as the raw- $CaCO_3$
16 nanoparticles (Fig. 2a), samples synthesized at RT (Fig. 2b) and samples
17 synthesized by AHT at 90 °C for 10 d (Fig. 2c) before acid treatment. This
18 verifies that the core nanoparticle ($CaCO_3$) was coated by amorphous silicate
19 (schematically shown in Fig. 1, 5).

20 But the AHT as-synthesized samples treated at 120 °C and aged for 10 d (Fig. 2d),
21 formed an additional sharp peak at ~ 18.1 (2θ). This peak corresponds to an
22 overlap diffraction peak of $Ca(OH)_2$ (Wang et al. 1997; Hong et al. 1999; Chen
23 et al. 2004; Kim et al. 2004; Qing et al. 2007) and is denoted as the low crystalline
24 phase of CSH, see Fig. S5 (Ishida et al. 1992b; Wang et al. 1997; Chen et al.
25 2004; Yanagisawa et al. 2006; Baltakys et al. 2007; Qing et al. 2007).

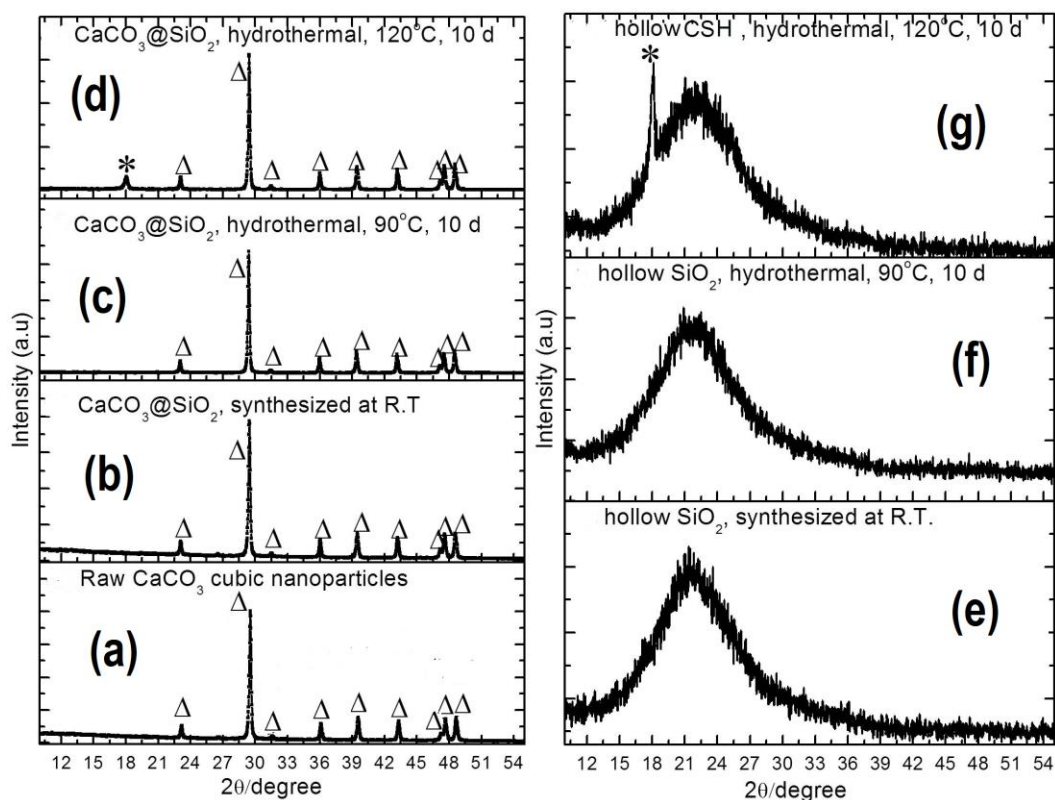
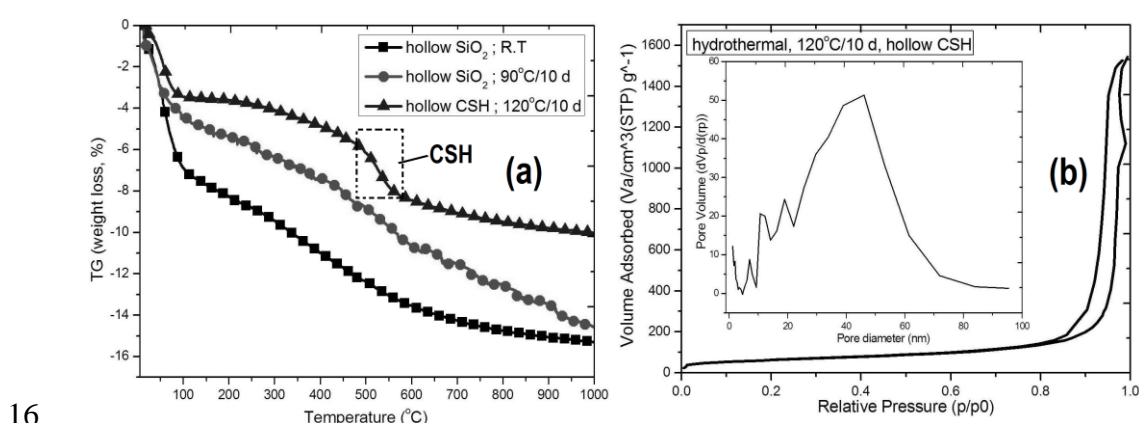


Fig. 2 XRD pattern of CaCO_3 (raw) nanoparticles (a), as synthesized samples at RT (b) and samples AHT aged for 10 d at 90 °C (c) and 120 °C (d). Then after acid treatment, formed an amorphous phase hollow samples (HS0dAH0ac (e) and HS10d90Hac (f)) except for sample CS10d120Hac (g). The (Δ) indicates the cubic calcite while (*) is the overlapped Ca(OH)_2 and semi-amorphous CSH phase , see Fig. S5

To confirm the formation of Ca(OH)_2 - SiO_{2-x} - H_2O system within the amorphous silicate-surface shell wall, an acid treatment was done for all the experimental samples for the dissolution of the CaCO_3 core-template nanoparticles. After acid etching, the reflection peak at ~ 18.1 (2θ) still existed for CS10d120Hac sample (see Fig. 2g, S5, S6), while no visual peaks (no other crystalline phases) were observed for the other samples such as the HS0dAH0ac (Fig.2e) and HS10d90Hac (Fig. 2f). Therefore, semi-amorphous CSH was contained in the shell wall of CS10d120Hac.

1 Thermal analysis and nitrogen adsorption-desorption isotherm

2 For confirmation, all synthesized hollow samples were subjected to
 3 thermogravimetric analysis (TG). As shown in Fig. 3a, a large gap of weight loss
 4 was detected between non-hydrothermal (HS0dAH0ac [■]) and AHT-treated
 5 hollow nanoparticles (HS10d90Hac [●] & CS10d120Hac [▲]). This was due to
 6 the removal of organic solvent and OH- groups (Kim et al. 2000; Li et al.2004). A
 7 slight drop in percentage weight loss at temperature (500 -600) °C was monitored
 8 for CS10d120Hac [▲] sample. This is due to the formation of new phase CSH
 9 during the synthesis of semi-amorphous CS10d120Hac (Ishida et al. 1992a, 1993;
 10 Saravanapavan et al. 2003; Brunner et al. 2006). These results are in-agreement
 11 with the XRD data obtained. In addition, the removal of organic solvent and OH
 12 groups accelerated during the AHT reaction. Structural re-arrangement within the
 13 amorphous silica shell occurred and led to the formation of (CS10d120Hac)
 14 hollow CSH with Ca(OH)₂ that was deposited onto the shell walls composed of
 15 silicate networks (Li et al. 1999,2002, 2004).



17 **Fig. 3** Thermogravimetric analysis (TG) (a) of the hollow samples namely HS0dAH0ac (■),
 18 HS10d90Hac (●) and CS10d120Hac (▲). Then in (b), N₂ adsorption desorption isotherm
 19 with inset pore (macro-pore) size distribution of CS10d120Hac particles (samples)

20
 21 For the surface area properties of the synthesized CS10d120Hac nanoparticles, N₂
 22 adsorption-desorption isotherm (77 K, Fig.3b) was used. Based from the isotherm

1 pattern, CS10d120Hac is classified as type II isotherm - adsorption-desorption
2 hysteresis with no plateau at high p/p_o (Sing et al. 1985). The steep increase at
3 p/p_o (0.9-1.0) denotes the macropore space in between the CS10d120Hac
4 nanoparticles or the macro-hole within the shell wall. The macropore space was
5 measured using Barrett-Joyner-Halenda (BJH) method ranging from (30 to 60)
6 nm based from the pore-space-size distribution curve pattern as shown in inset Fig.
7 3b. Then using Brunauer-Emmett-Tellers (BET) method, the specific surface area
8 of the CS10d120Hac samples was measured as $215.21 \text{ m}^2 \text{ g}^{-1}$. A slight difference
9 is observed, as compared to the HS0dAH0ac samples ($358.08 \text{ m}^2 \text{ g}^{-1}$, see Fig. S4).
10 The decrease in surface area of CS10d120Hac could be due to the thickening of
11 the silanol groups, which were developed during the formation of semi-
12 amorphous CSH phase framework with $\text{Ca}(\text{OH})_2$ that was present within the shell
13 wall (Lin et al. 1999; Wei et al. 2008). This improved the structural stability of the
14 nano-size CS10d120Hac particles within the shell wall which was composed of
15 ultra-fine micropores (Shin et al. 2003; Fuji et al. 2006, 2007).

16 **Structural and surface morphology**

17 The morphological profiles of the synthesized samples were observed by scanning
18 electron microscopy (SEM) and transmission electron microscopy (TEM). As
19 shown in Fig. 4, no major alteration was detected in terms of shape and size of
20 nanoparticles.

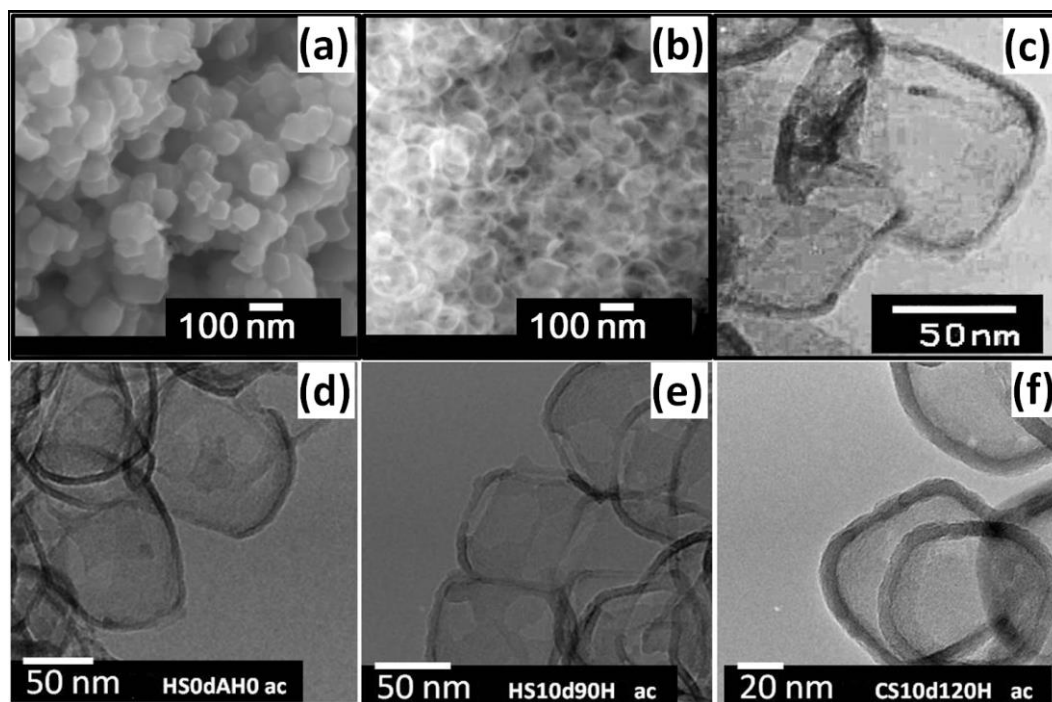


Fig. 4 SEM images of AHT synthesized sample at 120 °C for 10 d before (a) and after acid etch produced CS10d120Hac (b) with TEM images of CS10d120Hac (c, f), HS0dAH0ac (d) and HS10d90Hac (e)

The morphological shape of the samples was visibly preserved even after aging at ~120 °C for 10 d, as shown in Fig. 4a. After acid treatment, the hollow interior was clearly observed with hollow cavity size ranging from 60-100 nm and the uniform shell wall thickness approximately around ~10 nm as shown in SEM (Fig. 4b) and TEM images (Fig. 4c, 4f) for sample CS10d120Hac. These results were almost likely the same for the samples HS0dAH0ac (Fig. 4d) and HS10d90Hac (Fig. 4e) (see also Fig. S1, S2, S3).

Possible mechanism for the formation of semi-amorphous hollow calcium silicate hydrate nanoparticles via AHT method

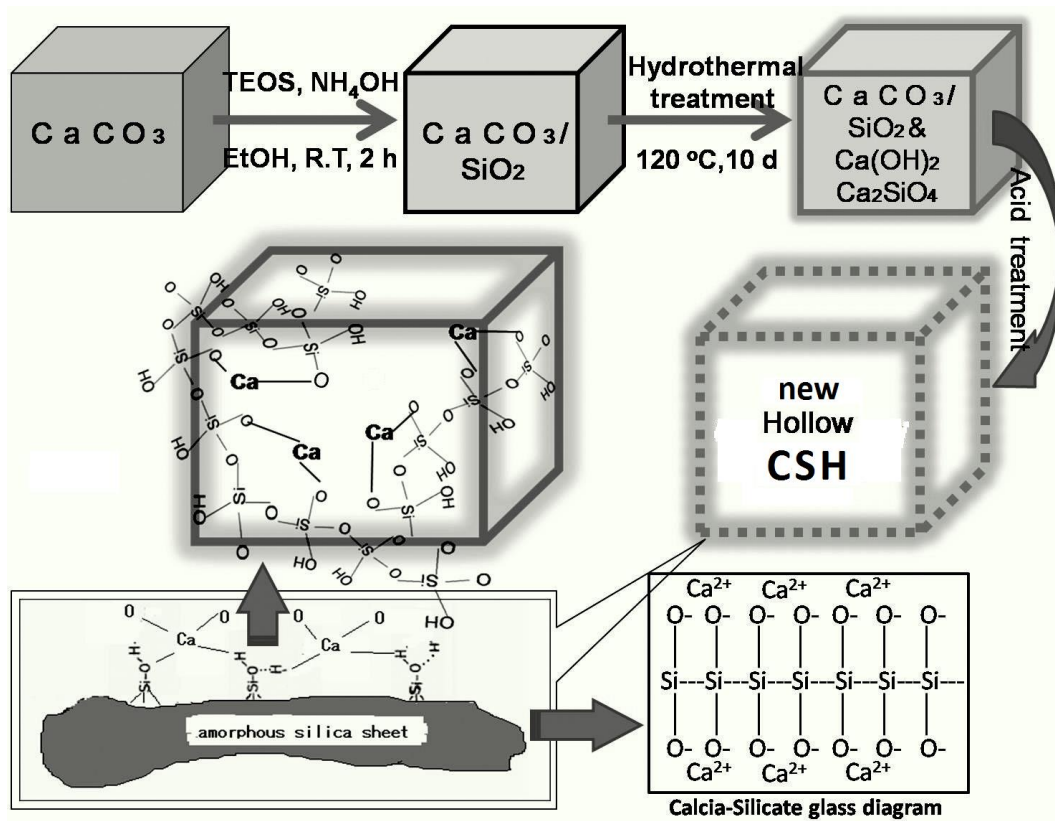
The formation of unique CS10d120Hac was attained by AHT at relatively low temperature reaction (i.e. 120 °C for 10 d) wherein the shell wall network structure of the synthesized hollow particles were composed of $\text{Ca}(\text{OH})_2$ and low

1 crystalline CSH (Wang et al. 1997; Chen et al. 2004; Yanagisawa et al. 2006;
2 Baltakys et al. 2007). Figure 5 illustrates the basic schematic plausible mechanism
3 for the formation of semi-amorphous hollow CSH nanoparticles by AHT with
4 aging. Upon increasing the reaction temperature of the AHT, the less-condensed
5 silicate species (Si-OH groups) can be subsequently re-arranged. Stabilization of
6 Si-OH groups occurred at this stage of the reaction. The $\text{Ca}(\text{OH})_2$ present on the
7 surfaces of CaCO_3 nanoparticles attached onto the exposed hydroxyl groups of the
8 silicate chains. At this critical point, the interaction between silicate (Si-OH) and
9 calcium hydroxide (Ca-OH) were transformed from a weaker electrostatic
10 interface (Si-OH-Ca) to a stronger electrostatic interaction (Si-O-Ca). A stable
11 phase of amorphous CSH systems was formed from AHT aging by deprotonation
12 caused by high pH (high alkaline) and high temperature (see Fig. S6). After acid
13 etching, hollow nanoparticles were produced wherein the thin-shell wall is
14 composed of semi-amorphous CSH (CS10d120Hac).

15 This process not only re-structures the silicate networks (ultra-microporous
16 structures) that led to the formation of semi-amorphous CSH with $\text{Ca}(\text{OH})_2$, but
17 also increased the thermal and hydrothermal stability of the nanostructure shell
18 wall (Lin et al. 1999, 2002; Park et al. 2001; Parfenov et al. 2003; Virtudazo et al.
19 2010). The nano-structural features of CS10d120Hac are highly desirable in
20 understanding the theoretical aspect of CSH nano-structure. The new synthesized
21 material exhibits a higher specific surface area and interconnected micropore
22 channels, which makes it worthy for drug loading and release applications.

23 Typically, the inner diameter and morphology of the unique CS10d120Hac can be
24 controlled by adopting varying sizes of CaCO_3 particles. In addition, further
25 characterization and experiment have been continuously done such as adjusting

1 the shell to mesoporous dimensions, varying the thickness, and incorporating
 2 other bio-active materials to the network.



3
 4 **Fig. 5** Schematic illustration and chemical reaction for the possible mechanism for the
 5 formation of hollow CSH nanoparticles (CS10d120Hac), see also Fig. S6

6 Conclusion

7 In this article, we demonstrated a simple method for the fabrication of semi-
 8 amorphous, nanosize CS10d120Hac ranging from 60-100 nm via AHT-aging
 9 process followed by acid treatment. The nanostructure shell stability of
 10 CS10d120Hac was dependent on the AHT reaction temperature and aging time. In
 11 future work, this material can be functionalized to form more dispersed particles
 12 and produce hollow hybrid bio-glass particles. Moreover, due to its exceptional
 13 specific surface area, porosity, and nanostructure, these may find wide use for
 14 varied applications such as in nano-cement, nano-biomedicine, and coating
 15 additives for thermal insulating materials.

1 **Conflict of interest**

2 The author declares that they have no competing interest.

3 **Authors Contributions**

4 RVRV carried out the experimentation, characterization and preparation of the manuscripts. M.F
5 and H.W guided the study, participated in the design, coordination and preparation of the
6 manuscripts. M.F and T.S assisted in guiding the experiment and coordinating and monitoring the
7 equipments during the research work. All the authors approved the final manuscript.

8 **Acknowledgements**

9 The authors gratefully acknowledge that this research was partially supported by the Japanese
10 Government Ministry of Education, Culture, Sports, Science and Technology (MEXT;
11 Monbukagakusho Scholarship) and Grant-in-Aid for Scientific Research 22310066 (2010-2012).
12 We are also thankful to C.C. Chua-Nakar (Reviewer-Inorganic Chemistry, Ramon Sison Review
13 Center) for the useful technical discussion and assistance with this study.

14 **Supplementary materials**

15 Supplementary materials (the abbreviation and further characterization details of the results on
16 SEM/TEM images, XRD analysis, Nitrogen adsorption desorption isotherms, detailed schematic
17 possible reactions of CS10d120Hac) is available in the online version of this article.

20 **References**

- 21
22 Allen AJ, Thomas JJ, Jennings HM (2007) Composition and density of nanoscale calcium-silicate-
23 hydrate in cement. *Nat Mater* 6 (4):311-316. doi:10.1038/nmat1871
24 Baltakys K, Jauberthie R, Siauciunas R, Kaminskas R (2007) Influence of modification of SiO₂ on
25 the formation of calcium silicate hydrate. *Mater Sci-Poland* 25 (3):663-670
26 Blakely CK, Bruno SR, Poltavets VV (2011) Low-temperature solvothermal approach to the
27 synthesis of La₄Ni₃O₈ by topotactic oxygen deintercalation. *Inorg Chem* 50 (14):6696-
28 6700. doi:10.1021/ic200677p
29 Brunner TJ, Grass RN, Stark WJ (2006) Glass and bioglass nanopowders by flame synthesis.
30 *Chem Commun (Camb)* (13):1384-1386. doi:10.1039/b517501a
31 Chang Y, Chen S, Cao A (2010) Mechanism of pressure-accelerated solvothermal reduction of
32 graphene oxide. *Journal of Shanghai University (Natural Science Edition)* 6:008.
33 doi:cnki:sun:sdxz.0.2010-06-008
34 Chen F, Zhu Y-J, Zhang K-H, Wu J, Wang K-W, Tang Q-L, Mo X-M (2011) Europium-doped
35 amorphous calcium phosphate porous nanospheres: preparation and application as
36 luminescent drug carriers. *Nanoscale Res Lett* 6 (1):67. doi:10.1186/1556-276x-6-67
37 Chen JJ, Thomas JJ, Taylor HFW, Jennings HM (2004) Solubility and structure of calcium silicate
38 hydrate. *Cem Concr Res* 34 (9):1499-1519. doi:10.1016/j.cemconres.2004.04.034
39 Chippindale AM, Cowley AR, Walton RI (1996) Solvothermal synthesis and structural
40 characterisation of the first ammonium cobalt gallium phosphate hydrate,
41 NH₄[CoGa₂P₃O₁₂(H₂O)₂]. *J Mater Chem* 6 (4):611-614. doi:10.1039/Jm9960600611
42 Coleman NJ, Bellantone M, Nicholson JW, Mendham AP (2007) Textural and structural
43 properties of bioactive glasses in the system CaO-SiO₂. *Ceramics Silikaty* 51 (1):1-8

- 1 Devaraju MK, Yin S, Sato T (2009) A fast and template free synthesis of Tb:Y₂O₃ hollow
2 microspheres via supercritical solvothermal method. Cryst Growth Des 9 (6):2944-2949.
3 doi:10.1021/cg9002934
- 4 Fuji M, Shin T, Watanabe H, Takei T (2012) Shape-controlled hollow silica nanoparticles
5 synthesized by an inorganic particle template method. Adv Powder Technol 23 (5):562-
6 565. doi:10.1016/j.appt.2011.06.002
- 7 Fuji M, Takai C, Takahashi M (2005) Synthesis of Nano-size hollow particles and its application.
8 In: The 2006 Spring National Meeting, 2006
- 9 Fuji M, Takai C, Tarutani Y, Takei T, Takahashi M (2007) Surface properties of nanosize hollow
10 silica particles on the molecular level. Adv Powder Technol 18 (1):81-91.
11 doi:10.1163/156855207779768124
- 12 Gandolfi MG, Ciapetti G, Taddei P, Perut F, Tinti A, Cardoso MV, Van Meerbeek B, Prati C
13 (2010) Apatite formation on bioactive calcium-silicate cements for dentistry affects
14 surface topography and human marrow stromal cells proliferation. Dent Mater 26
15 (10):974-992. doi:10.1016/j.dental.2010.06.002
- 16 Gou Z, Chang J (2004) Synthesis and in vitro bioactivity of dicalcium silicate powders. J Eur
17 Ceram Soc 24 (1):93-99. doi:10.1016/s0955-2219(03)00320-0
- 18 Hong S-H, Young JF (1999) Hydration Kinetics and Phase Stability of Dicalcium Silicate
19 Synthesized by the Pechini Process. J Am Ceram Soc 82 (7):1681-1686.
20 doi:10.1111/j.1151-2916.1999.tb01986.x
- 21 Hoshino S, Yamada K, Hirao H (2006) XRD/Rietveld analysis of the hydration and strength
22 development of slag and limestone blended cement. Journal of Advanced Concrete
23 Technology 4 (3):357-367. doi:dx.doi.org/10.3151/jact.4.357
- 24 Huang X, Jiang D, Tan S (2002) Novel hydrothermal synthesis method for tobermorite fibers and
25 investigation on their thermal stability. Mater Res Bull 37 (11):1885-1892.
26 doi:10.1016/s0025-5408(02)00854-1
- 27 Ishida H, Mabuchi K, Sasaki K, Mitsuda T (1992a) Low-temperature synthesis of β -Ca₂SiO₄ from
28 Hillebrandite. J Am Ceram Soc 75 (9):2427-2432. doi:10.1111/j.1151-
29 2916.1992.tb05595.x
- 30 Ishida H, Sasaki K, Mitsuda T (1992b) Highly reactive β -Dicalcium silicate: I, hydration behavior
31 at room temperature. J Am Ceram Soc 75 (2):353-358. doi:10.1111/j.1151-
32 2916.1992.tb08186.x
- 33 Ishida H, Yamazaki S, Sasaki K, Okada Y, Mitsuda T (1993) α -Dicalcium silicate hydrate:
34 preparation, decomposed phase, and its hydration. J Am Ceram Soc 76 (7):1707-1712.
35 doi:10.1111/j.1151-2916.1993.tb06638.x
- 36 Kim JA, Suh JK, Jeong SY, Lee JM, Ryu SK (2000) Hydration reaction in synthesis of crystalline-
37 layered sodium silicate. J Ind Eng Chem 6 (4):219-225
- 38 Kim Y-M, Hong S-H (2004) Influence of minor ions on the stability and hydration rates of β -
39 dicalcium silicate. J Am Ceram Soc 87 (5):900-905. doi:10.1111/j.1151-
40 2916.2004.00900.x
- 41 Li H, Chang J (2005) Preparation, characterization and in vitro release of gentamicin from
42 PHBV/wollastonite composite microspheres. J Controlled Release 107 (3):463-473.
43 doi:10.1016/j.jconrel.2005.05.019
- 44 Li XK, Chang J (2004) Synthesis of wollastonite single crystal nanowires by a novel hydrothermal
45 route. Chem Lett 33 (11):1458-1459. doi:10.1246/cl.2004.1458
- 46 Lin HP, Mou CY (2002) Salt effect in post-synthesis hydrothermal treatment of MCM-41.
47 Micropor Mesopor Mat 55 (1):69-80. doi:10.1016/s1387-1811(02)00407-9
- 48 Lin HP, Mou CY, Liu SB (1999) Ammonia hydrothermal treatment on mesoporous silica structure
49 synthesized from acidic route. Chem Lett (12):1341-1342. doi:10.1246/Cl.1999.1341
- 50 Lin HP, Mou CY, Liu SB (2000) Formation of mesoporous silica nanotubes. Adv Mater 12
51 (2):103-106. doi:10.1002/(sici)1521-4095(200001)12:2<103::aid-adma103>3.0.co;2-p
- 52 Lin HP, Mou CY, Liu SB, Tang CY, Lin CY (2001) Post-synthesis treatment of acid-made
53 mesoporous silica materials by ammonia hydrothermal process. Micropor Mesopor Mat
54 44-45:129-137. doi:10.1016/s1387-1811(01)00176-7
- 55 Mitsuda T, Toraya H (1986) Hydrothermally formed γ -Ca₂SiO₄: Cell parameters and
56 thermogravimetry. Cem Concr Res 16 (1):105-110. doi:10.1016/0008-8846(86)90074-8
- 57 Nicoleau L (2010) New calcium silicate hydrate network. Transportation Research Record:
58 Journal of the Transportation Research Board 2142 (1):42-51. doi:10.3141/2142-07
- 59 Okada Y, Ishida H, Sasaki K, Young JF, Mitsuda T (1994) Characterization of C-S-H from highly
60 reactive β -dicalcium silicate prepared from Hillebrandite. J Am Ceram Soc 77 (5):1313-
61 1318. doi:10.1111/j.1151-2916.1994.tb05408.x

- 1 Parfenov VA, Kirik SD (2003) Effect of reaction medium on hydrothermal stability of
2 mesostructured silicate material MCM-41. *Chemistry for Sustainable Development*
3 11:735-740
- 4 Park DH, Nishiyama N, Egashira Y, Ueyama K (2001) Enhancement of hydrothermal stability and
5 hydrophobicity of a silica MCM-48 membrane by silylation. *Ind Eng Chem Res* 40
6 (26):6105-6110. doi:10.1021/ie0103761
- 7 Pei LZ, Yang LJ, Yang Y, Fan CG, Yin WY, Chen J, Zhang QF (2010) A green and facile route to
8 synthesize calcium silicate nanowires. *Mater Charact* 61 (11):1281-1285.
9 doi:10.1016/j.matchar.2010.07.002
- 10 Qing Y, Zenan Z, Deyu K, Rongshen C (2007) Influence of nano-SiO₂ addition on properties of
11 hardened cement paste as compared with silica fume. *Construction and Building*
12 *Materials* 21 (3):539-545. doi:10.1016/j.conbuildmat.2005.09.001
- 13 Ríos CA, Williams CD, Fullen MA (2009) Hydrothermal synthesis of hydrogarnet and tobermorite
14 at 175 °C from kaolinite and metakaolinite in the CaO–Al₂O₃–SiO₂–H₂O system: A
15 comparative study. *Applied Clay Science* 43 (2):228-237. doi:10.1016/j.clay.2008.09.014
- 16 Saravanapavan P, Hench LL (2003) Mesoporous calcium silicate glasses. I. Synthesis. *J Non-Cryst*
17 *Solids* 318 (1–2):1-13. doi:10.1016/s0022-3093(02)01864-1
- 18 Saravanapavan P, Jones JR, Pryce RS, Hench LL (2003) Bioactivity of gel–glass powders in the
19 CaO–SiO₂ system: A comparison with ternary (CaO–P₂P₅–SiO₂) and quaternary glasses
20 (SiO₂–CaO–P₂O₅–Na₂O). *Journal of biomedical materials research Part A* 66A (1):110-
21 119. doi:10.1002/jbm.a.10532
- 22 Shin T, Fuji M, Takei T, Chikazawa K, Tanabe K, Mitsuhashi K Evaluation of structure of silica
23 nano hollow particles prepared with fine calcium carbonate particles as a template. In:
24 *Proc. of 83rd Annual Meeting of the Chemical Society of Japan*, 2003. p 366
- 25 Sing KSW, Everett DH, Haul RAW, Moscou L, Pierotti RA, Rouquerol J, Siemieniowska T
26 (1985) Reporting physisorption data for gas/solid systems with special reference to the
27 determination of surface-area and porosity. *Pure Appl Chem* 57 (4):603-619.
28 doi:10.1351/pac198557040603
- 29 Takagi M, Maeda H, Ishida EH (2009) Hydrothermal solidification of green tuff / tobermorite
30 composites. *J Ceram Soc Jpn* 117 (1371):1221-1224.
31 doi:dx.doi.org/10.2109/jcersj2.117.1221
- 32 Takai C, Fuji M, Fujimoto K (2011) Skeletal silica nanoparticles prepared by control of reaction
33 polarity. *Chem Lett* 40 (12):1346-1348. doi:10.1246/Cl.2011.1346
- 34 Taylor H FW (1986) Proposed structure for calcium silicate hydrate gel. *J Am Ceram Soc* 69
35 (6):464-467. doi:10.1111/j.1151-2916.1986.tb07446.x
- 36 Udawatte CP, Yanagisawa K, Kamakura T, Matsumoto Y, Yamasaki N (2000) Solidification of
37 xonotlite fibers with chitosan by hydrothermal hot pressing. *Mater Lett* 45 (6):298-301.
38 doi:10.1016/s0167-577x(00)00121-x
- 39 Virtudazo RV, Rivera, Watanabe H, Fuji M, Takahashi M (2010) A simple approach to form
40 hydrothermally stable templated hollow silica nanoparticles. In: Ewsuk K, Naito M,
41 Kakeshita T, Kirihara S, Uematsu K, Abe H (eds) *Characterization and Control of*
42 *Interfaces for High Quality Advanced Materials III*. John Wiley & Sons, Inc., NJ, USA,
43 pp 91-97. doi:10.1002/9780470917145.ch14
- 44 Wang J, Tomita A (1997) Hydrothermal reaction of Ca(OH)₂ with quartz in connection with coal
45 demineralization. *Ind Eng Chem Res* 36 (5):1464-1469. doi:10.1021/ie960516k
- 46 Watanabe O, Kitamura K, Maenami H, Ishida H (2001) Hydrothermal treatment of a silica sand
47 complex with lime. *J Am Ceram Soc* 84 (10):2318-2322. doi:10.1111/j.1151-
48 2916.2001.tb01008.x
- 49 Wei Q, Wang F, Nie ZR, Song CL, Wang YL, Li QY (2008) Highly hydrothermally stable
50 microporous silica membranes for hydrogen separation. *The journal of physical chemistry*
51 *B* 112 (31):9354-9359. doi:10.1021/jp711573f
- 52 Wu J, Zhu YJ, Cao SW, Chen F (2010) Hierachically nanostructured mesoporous spheres of
53 calcium silicate hydrate: surfactant-free sonochemical synthesis and drug-delivery system
54 with ultrahigh drug-loading capacity. *Adv Mater* 22 (6):749-753.
55 doi:10.1002/adma.200903020
- 56 Yanagisawa K, Hu X, Onda A, Kajiyoshi K (2006) Hydration of β-dicalcium silicate at high
57 temperatures under hydrothermal conditions. *Cem Concr Res* 36 (5):810-816.
58 doi:10.1016/j.cemconres.2005.12.009
- 59 Zhang M, Chang J (2010) Surfactant-assisted sonochemical synthesis of hollow calcium silicate
60 hydrate (CSH) microspheres for drug delivery. *Ultrason Sonochem* 17 (5):789-792.
61 doi:10.1016/j.ultsonch.2010.01.012
- 62

1
2
3
4
5
6
7
8
9
10
11
12
13
14
15
16
17
18
19
20
21
22
23
24
25
26
27
28
29
30
31
32
33
34
35
36
37

**Simple preparation and initial characterization
of semi-amorphous hollow calcium silicate
hydrate nanoparticles by ammonia-
hydrothermal-template techniques**

Raymond V.Rivera Virtudazo, Hideo Watanabe, Takashi Shirai, Masayoshi Fuji*

*Advanced Ceramics Research Center, Nagoya Institute of Technology,
Crystal Plaza 4F, 3-101-1 Honmachi, Tajimi, Gifu 507-0033 Japan*

Tel.: +81-572-24-8110
Fax: +81-572-24-8109
*corresponding author: fuji@nitech.ac.jp

Email addresses:
RVRV: raymond@crl.nitech.ac.jp or rrvrv26@gmail.com
H.W: hideo.watanabe@gmail.com
T.S: shirai@nitech.ac.jp
M.F: fuji@nitech.a.jp

FIGURE CAPTIONS

Fig. 1 Process flow with an illustration of the simple set-up of AHT (f) during the synthesis of CS10d120Hac: **a** proportioning; **b** mixing for hydrolysis and condensation to form core-shell nanoparticles ($\text{CaCO}_3 @ \text{SiO}_2 \cdot n\text{H}_2\text{O}$); **c** subjected to AHT at varying temperature for 10 days; **d** Dried and acid etched to remove CaCO_3 nanoparticles templates; **e** then obtain CS10d120Hac

Fig. 2 XRD pattern of CaCO_3 (raw) nanoparticles (**a**), as synthesized samples at RT (**b**) and samples AHT aged for 10 d at 90 °C (**c**) and 120 °C (**d**). Then after acid treatment, formed an amorphous phase hollow samples (HS0dAH0ac (**e**) and HS10d90Hac (**f**)) except for sample CS10d120Hac (**g**). The (Δ) indicates the cubic calcite while (*) is the overlapped $\text{Ca}(\text{OH})_2$ and semi-amorphous CSH phase, see Fig. S5

Fig. 3 Thermogravimetric analysis (TG) (**a**) of the hollow samples namely HS0dAH0ac (\blacksquare), HS10d90Hac (\bullet) and CS10d120Hac (\blacktriangle). Then in (**b**), N_2 adsorption desorption isotherm with inset pore (macro-pore) size distribution of CS10d120Hac particles (samples)

Fig. 4 SEM images of AHT synthesized sample at 120 °C for 10 d before (**a**) and after acid etch produced CS10d120Hac (**b**) with TEM images of CS10d120Hac (**c, f**), HS0dAH0ac (**d**) and HS10d90Hac (**e**)

Fig. 5 Schematic illustration and chemical reaction for the possible mechanism for the formation of hollow CSH nanoparticles (CS10d120Hac), see also Fig. S6

FIGURES

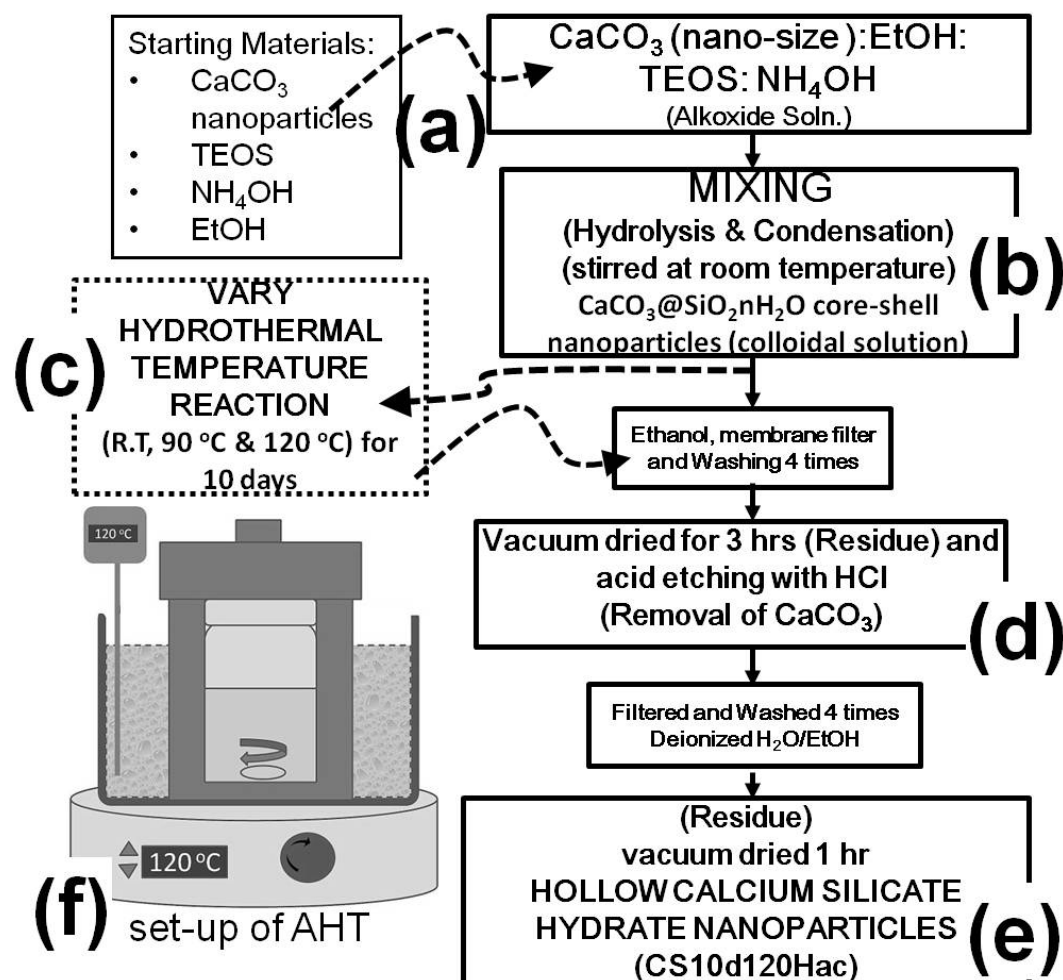


Fig. 1 Process flow with an illustration of the simple set-up of AHT (f) during the synthesis of CS10d120Hac: **a** proportioning; **b** mixing for hydrolysis and condensation to form core-shell nanoparticles ($\text{CaCO}_3 @ \text{SiO}_2 \cdot n\text{H}_2\text{O}$); **c** subjected to AHT at varying temperature for 10 days; **d** Dried and acid etched to remove CaCO_3 nanoparticles templates; **e** then obtain CS10d120Hac

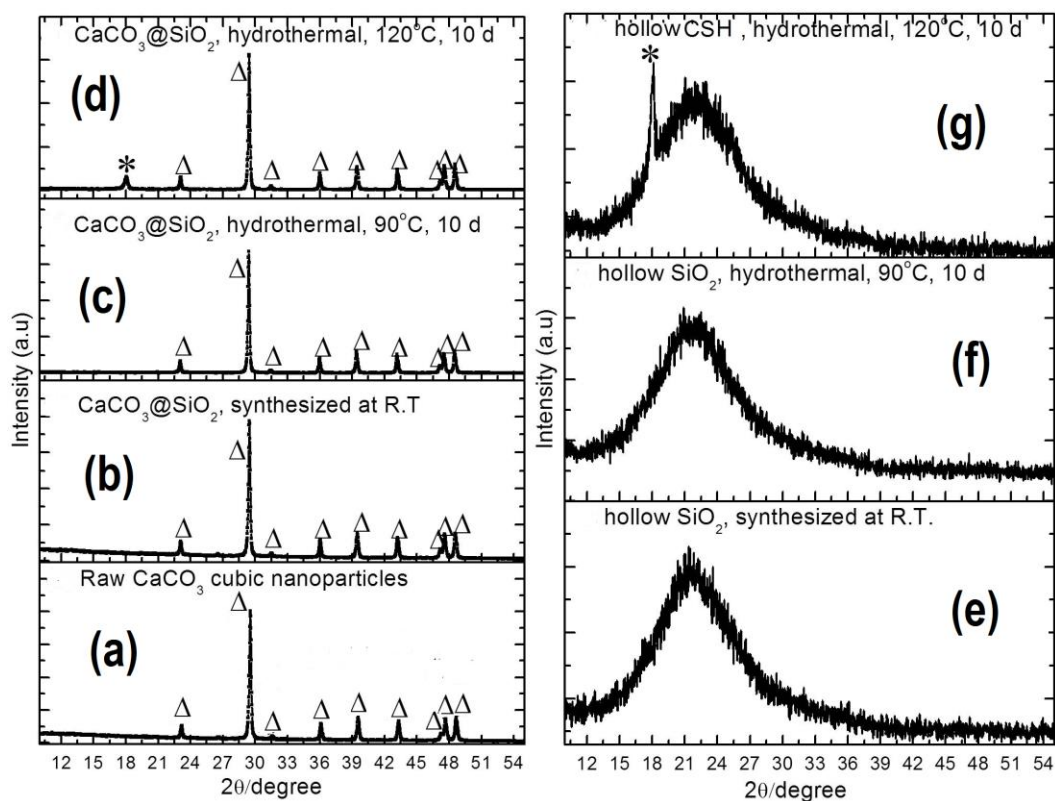


Fig. 2 XRD pattern of CaCO_3 (raw) nanoparticles (a), as synthesized samples at RT (b) and samples AHT aged for 10 d at 90 °C (c) and 120 °C (d). Then after acid treatment, formed an amorphous phase hollow samples (HS0dAH0ac (e) and HS10d90Hac (f)) except for sample CS10d120Hac (g). The (Δ) indicates the cubic calcite while (*) is the overlapped Ca(OH)_2 and semi-amorphous CSH phase, see Fig. S5

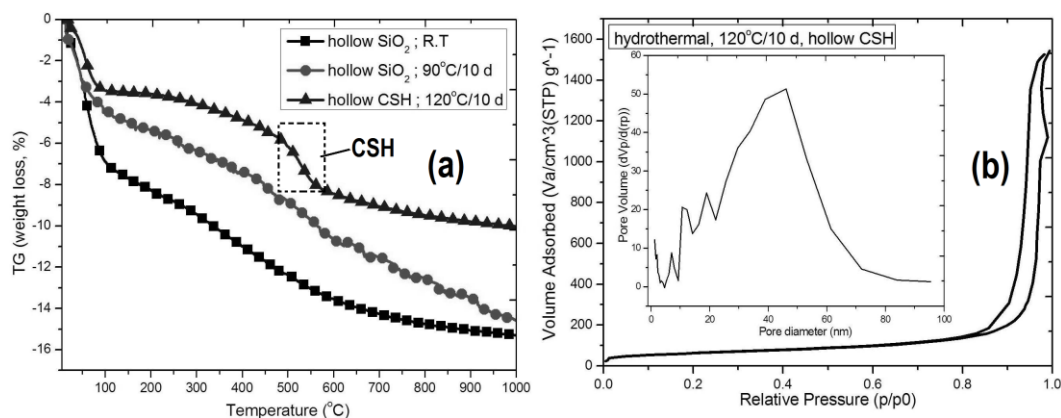


Fig. 3 Thermogravimetric analysis (TG) (a) of the hollow samples namely HS0dAH0ac (■), HS10d90Hac (●) and CS10d120Hac (▲). Then in (b), N₂ adsorption-desorption isotherm with inset pore (macro-pore) size distribution of CS10d120Hac particles (samples)

1
2
3
4
5
6
7
8
9
10
11
12
13
14
15
16
17
18
19
20
21

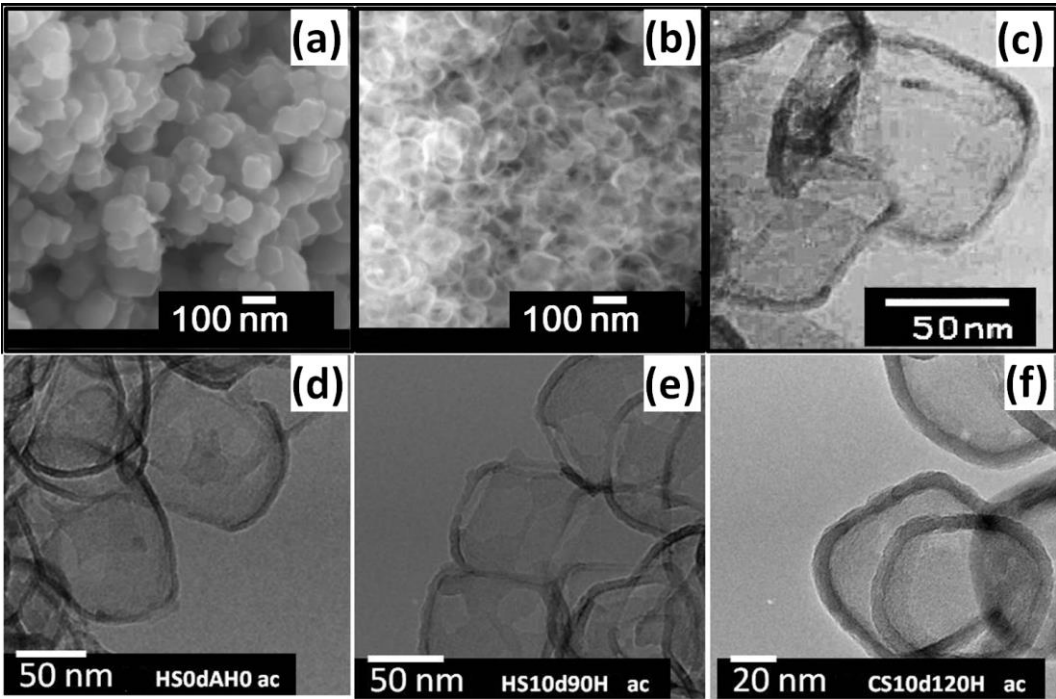


Fig. 4 SEM images of AHT synthesized sample at 120 °C for 10 d before (a) and after acid etch produced CS10d120Hac (b) with TEM images of CS10d120Hac (c, f), HS0dAH0ac (d) and HS10d90Hac (e)

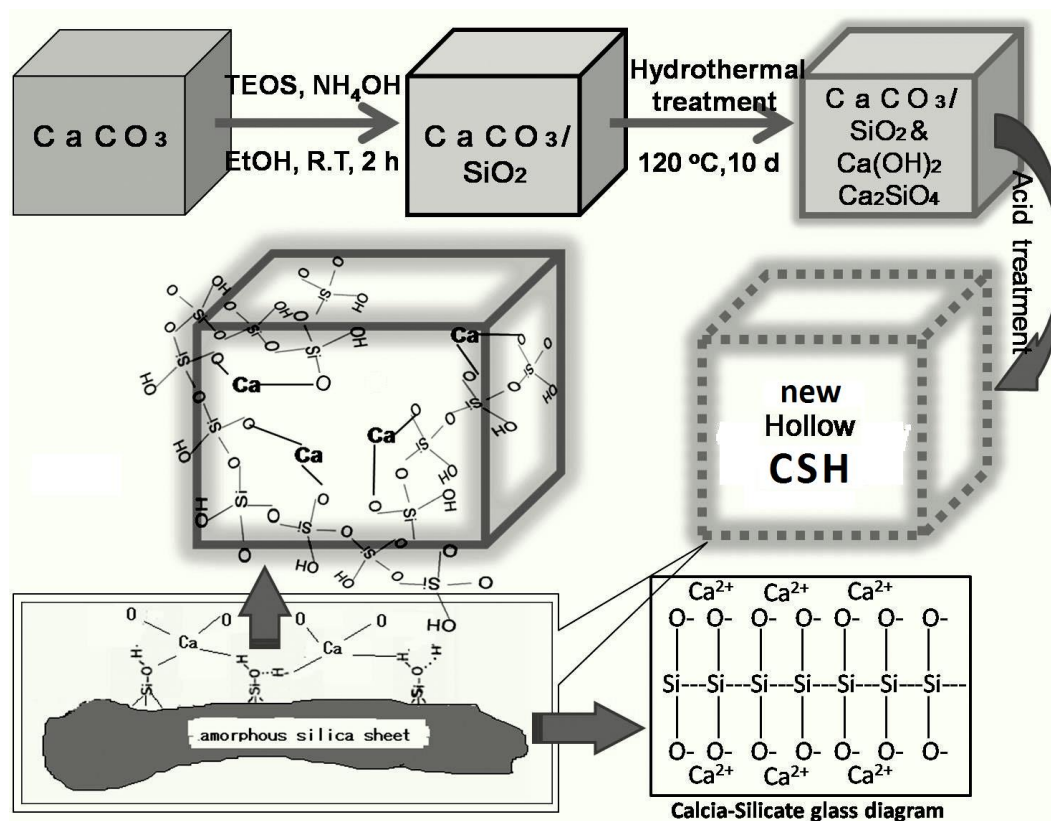


Fig. 5 Schematic illustration and chemical reaction for the possible mechanism for the formation of hollow CSH nanoparticles (CS10d120Hac), see also Fig. S6

1 Supporting information

2 **Simple preparation and initial characterization**
3 **of semi-amorphous hollow calcium silicate**
4 **hydrate nanoparticles by ammonia-**
5 **hydrothermal-template techniques**

6 Raymond V.Rivera Virtudazo, Hideo Watanabe, Takashi Shirai, Masayoshi Fuji*

7 *Advanced Ceramics Research Center, Nagoya Institute of Technology,*
8 *Crystal Plaza 4F, 3-101-1 Honmachi, Tajimi, Gifu 507-0033 Japan*

9 Tel.: +81-572-24-8110

10 Fax: +81-572-24-8109

11 *corresponding author: fuji@nitech.ac.jp

12

13 Email addresses:

14 RVRV: raymond@crl.nitech.ac.jp or rrvv26@gmail.com

15 H.W: hideo.watanabe@gmail.com

16 T.S: shirai@nitech.ac.jp

17 M.F: fuji@nitech.a.jp

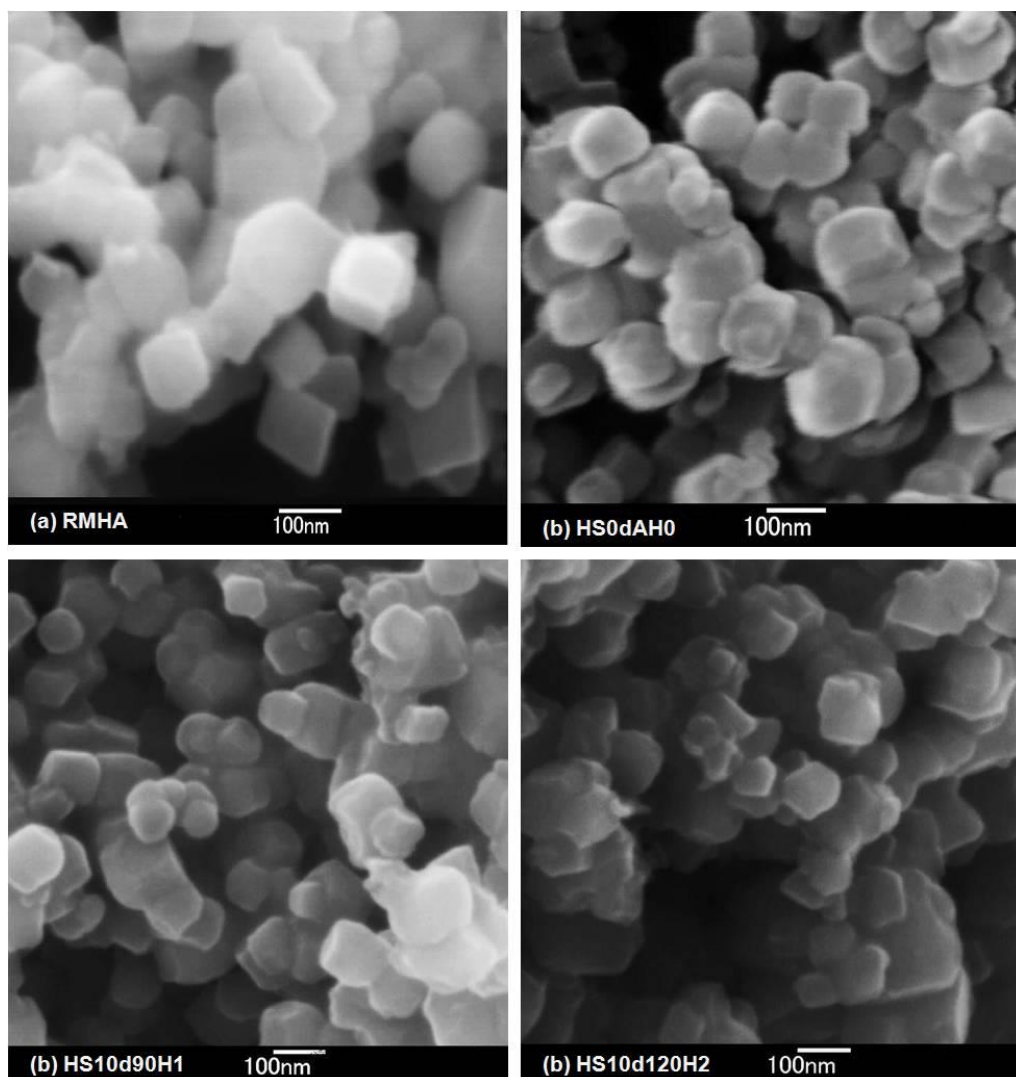
18

19

20 **ABBREVIATIONS**

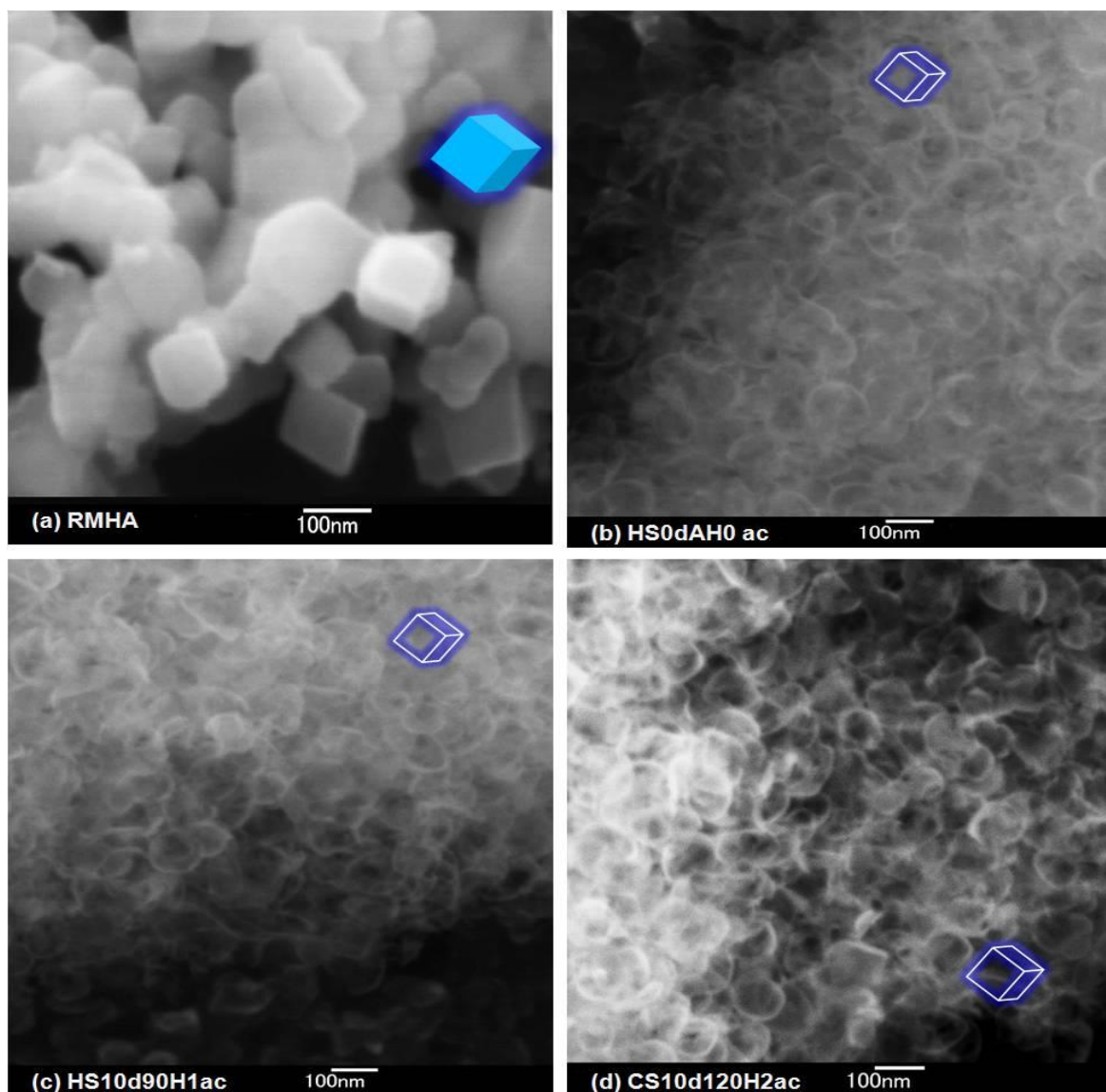
21 CSH, CC calcium silicate hydrates; RT, CC room temperature; HP, CC
22 hydrothermal process; DDA, CC drug delivery application; CS10d120Hac, CC
23 hollow CSH nanoparticles; CaCO₃@SiO₂, CC calcium carbonate & silicate
24 core-shell; SC, CC solvothermal concept; EtOH, CC ethanol; AHT, CC
25 ammonia-hydrothermal technique; Ca(OH)₂, CC calcium hydroxide; CaCO₃, CC
26 calcium carbonate, SiO₂, CC silica, silicate; TEOS, CC tetraethyl orthosilicate;
27 XRD, CC x-ray diffraction; NH₄ (aq), ammonia solution; HS0DAHac, CC hollow
28 SiO₂ nanoparticles non-AHT treatment; HS10d90Hac, CC hollow SiO₂
29 nanoparticles AHT treated for 10 d at 90°C; SEM, CC scanning electron
30 microscopy; TEM, CC transmission electron microscope; TG, CC
31 thermogravimetric analysis; BJH, CC Barrett-Joyner-Halenda method; BET, CC
32 Brunauer-Emmett-Tellers Method.

1 Results



2
3 **Fig. S1** SEM images of before acid treatment : (a) CaCO_3 raw (RMHA) , (b)
4 CaCO_3 coated with SiO_2 without hydrothermal (HS0dAH0) , (c) CaCO_3 coated
5 with SiO_2 by hydrothermal at 90 °C for 10 d (HS10d90H1), (d) CaCO_3 coated
6 with SiO_2 by hydrothermal at 120 °C for 10 d (CS10d120H2).

7



1
2 **Fig. S2** SEM images: (a) [RMHA] CaCO_3 raw; after acid treated samples (b)
3 (HS0dAH0ac) nano-size hollow SiO_2 without hydrothermal, (c) (HS10d90H1ac)
4 nano-size hollow SiO_2 by hydrothermal at 90 °C for 10 d (d) (CS10d120Hac)
5 nano-size hollow CSH with hydrothermal at 120 °C for 10 d.

6

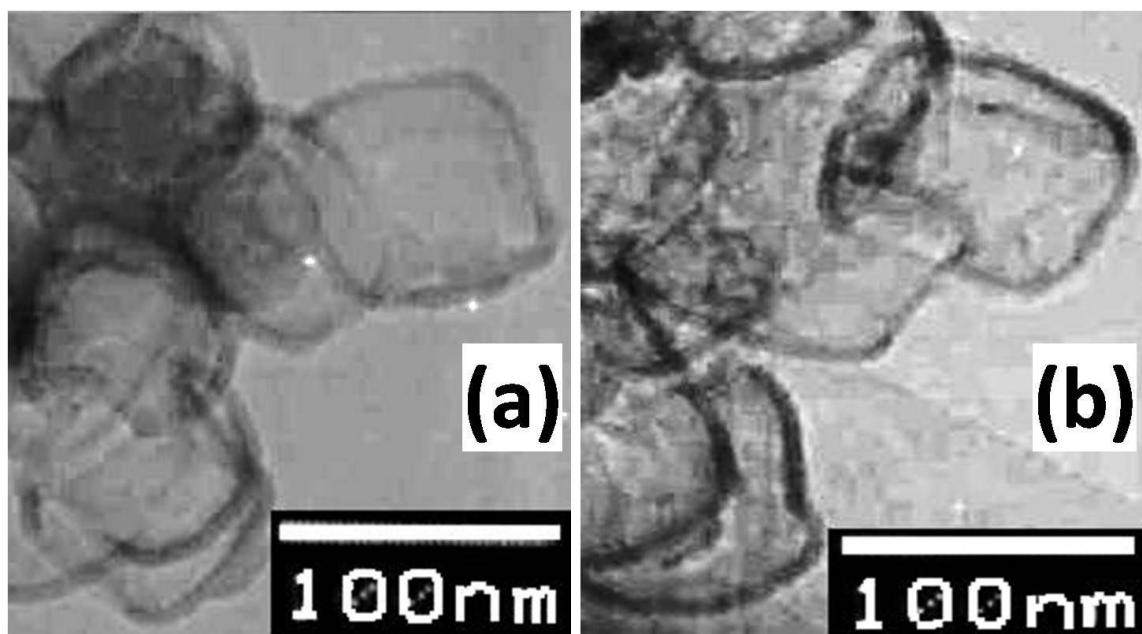


Fig. S3 TEM images: Acid treated samples (a) (HS0dAH0ac) nano-size hollow SiO_2 without hydrothermal, (b) (CS10d120Hac) nano-size hollow CSH with hydrothermal at 120 °C for 10 d.

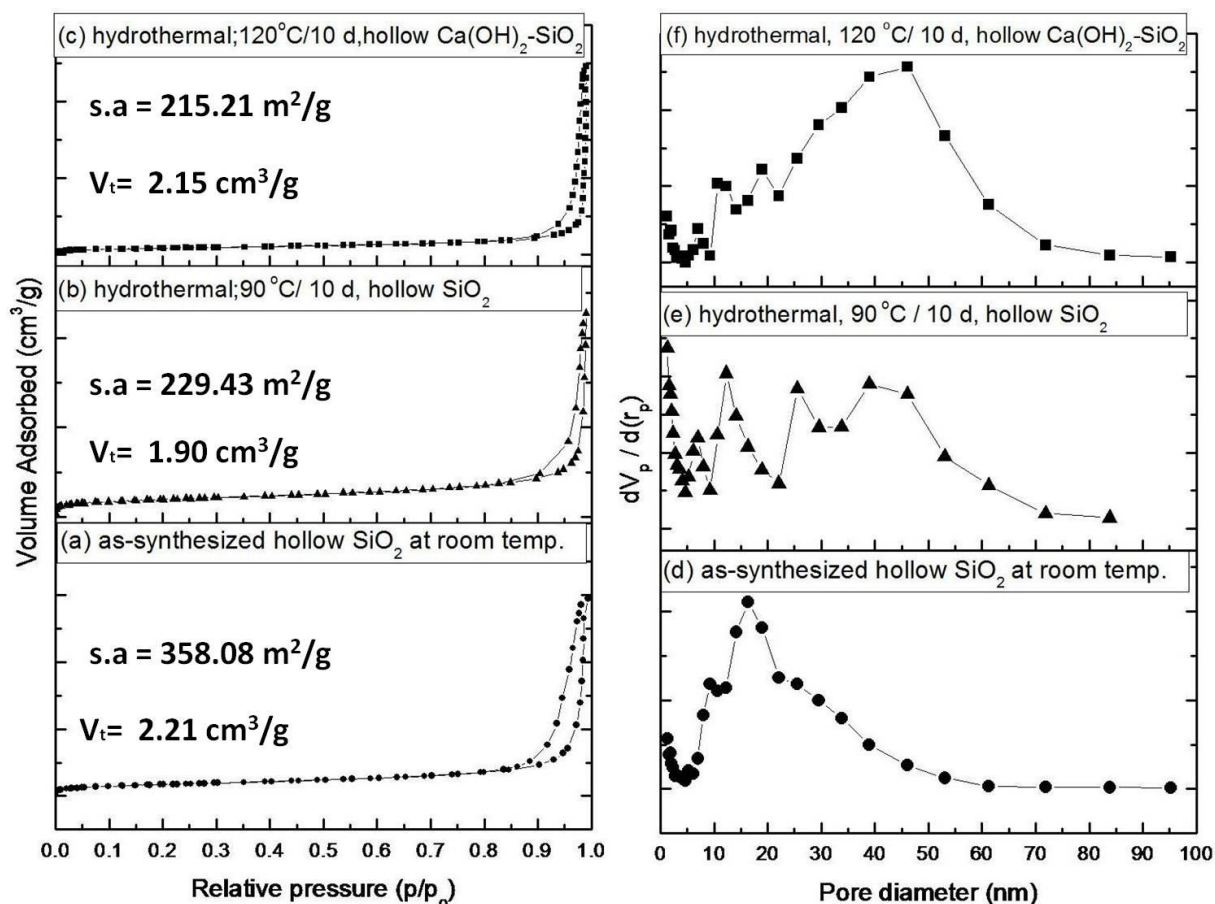


Fig. S4 Nitrogen adsorption-desorption isotherms (a to c) and BJH differential pore size distribution (d to f) of hollow particles synthesized at ambient temperature (HS0dAH0ac), hollow particles hydrothermally treated at 90°C for 10 d (HS10d90Hac) and hollow calcia-silicate nano particles hydrothermally treated at 120°C for 10 d (CS10d120Hac).

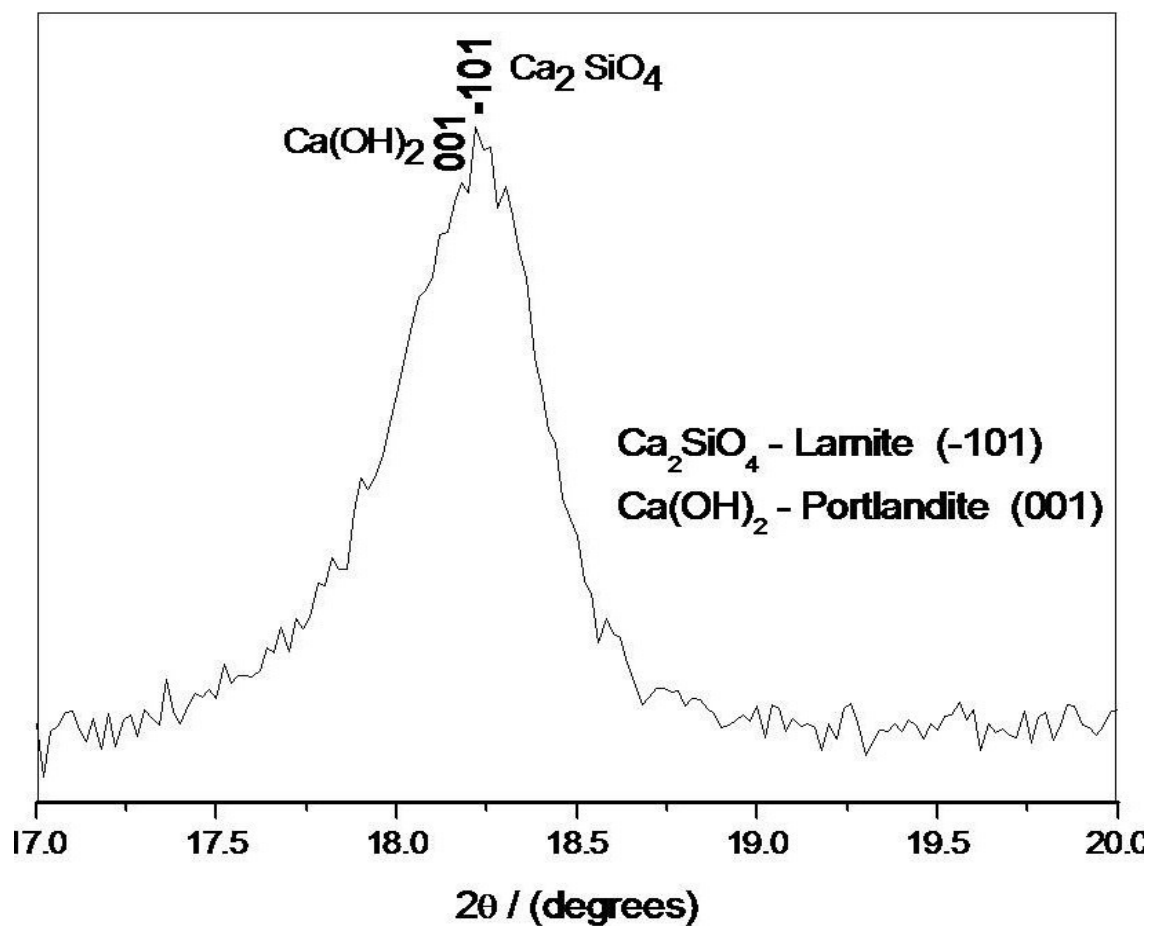
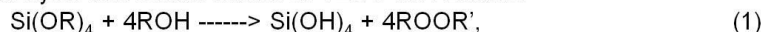


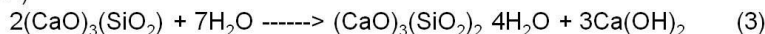
Fig. S5 Enlarge XRD of (CS10d120Hac) hollow CSH nanoparticles hydrothermally treated at 120 °C for 10 d ranging from (17.0 to 20.0) 2θ . [1-3]

POSSIBLE CHEMICAL REACTIONS:

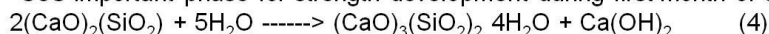
- Hydrolysis and condensation of TEOS with Ethanol



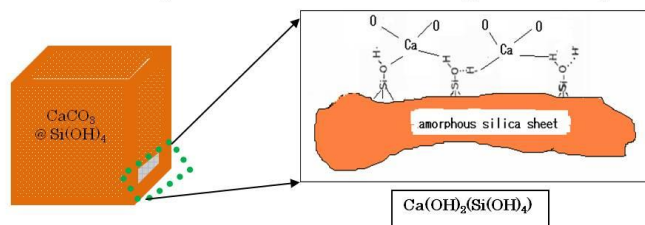
- Silicate phases reacts with water to form calcium hydroxide and rigid calcium-silicate hydrate gel (CSH)



*C3S important phase for strength development during first month of cement

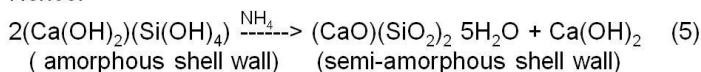


*C2S slowly reacts and contributes long-term strength of cement

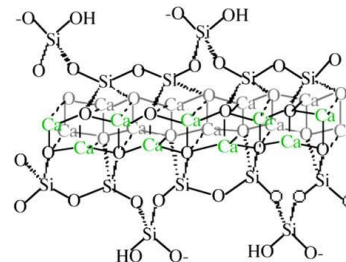
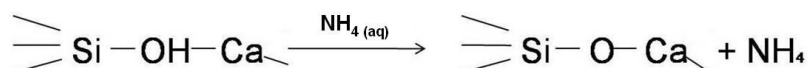


(Note: CaCO_3 surfaces has Ca(OH)_2)

Hence:



For simplicity:



Typical CSH materials, viewed along a polysilicate chain. Silicate ions either share oxygen atoms with central CaO_2 core or bridge silicate tetrahedral. Interlayer calcium ions and water molecules are omitted for clarity

Fig. S6 Possible chemical scheme for the formation of hollow CSH nanoparticles

References:

- Fuji M, Takai C, Takahashi M (2005) Synthesis of Nano-size hollow particles and its application. In: The 2006 Spring National Meeting, 2006
- Fuji M, Takai C, Tarutani Y, Takei T, Takahashi M (2007) Surface properties of nanosize hollow silica particles on the molecular level. Adv Powder Technol 18 (1):81-91. doi: 10.1163/156855207779768124
- Hoshino S, Yamada K, Hirao H (2006) XRD/Rietveld Analysis of the Hydration and strength development of slag and limestone blended cement. Journal of Advanced Concrete Technology 4 (3):357-367
- Huang X, Jiang D, Tan S (2002) Novel hydrothermal synthesis method for tobermorite fibers and investigation on their thermal stability. Mater Res Bull 37 (11):1885-1892. doi:10.1016/s0025-5408(02)00854-1
- Kim JA, Suh JK, Jeong SY, Lee JM, Ryu SK (2000) Hydration Reaction in Synthesis of Crystalline-Layered Sodium Silicate. J Ind Eng Chem 6 (4): 219-225
- Li X, Chang J (2004) Synthesis of Wollastonite Single Crystal Nanowires by a Novel Hydrothermal Route. Chem Lett 33 (11):1458-1459
- Qing Y, Zenan Z, Deyu K, Rongshen C (2007) Influence of nano-SiO₂ addition on properties of hardened cement paste as compared with silica fume. Construction and Building Materials 21 (3):539-545

1 Shin T, Fuji M, Takei T, Chikazawa K, Tanabe K, Mitsunashi K Evaluation of structure of silica
2 nano hollow particles prepared with fine calcium carbonate particles as a template. In:
3 Proc. of 83rd Annual Meeting of the Chemical Society of Japan, 2003. p 366
4 Tsurumi T, Hirano Y, Kato H, Kamiya T, Daimon M (1993) Crystal structure and hydration of
5 belite. Ceram Trans 40:19-25
6
7
8
9
10
11
12
13
14
15